The lower limit for time resolution in frequency modulation atomic force microscopy

Zeno Schumacher,* Andreas Spielhofer, Yoichi Miyahara, and Peter Grutter

Department of Physics, McGill University, Montreal, Quebec, Canada H3A 2T8

(Dated: August 22, 2016)

Atomic force microscopy (AFM) routinely achieves structural information in the sub-nm length scale. Measuring time resolved properties on this length scale to understand kinetics at the nm scale remains an elusive goal. We present a general analysis of the lower limit for time resolution in AFM. Our finding suggests the time resolution in AFM is ultimately limited by the well-known thermal limit of AFM and not as often proposed by the mechanical response time of the force sensing cantilever. We demonstrate a general pump-probe approach using the cantilever as a detector responding to the averaged signal. This method can be applied to any excitation signal such as electrical, thermal, magnetic or optical. Experimental implementation of this method allows us to measure a photocarrier decay time of ~ 1 ps in low temperature grown GaAs using a cantilever with a resonance frequency of 280 kHz.

INTRODUCTION

Understanding structure-function relations at the nanometer length scale is important for many fundamental as well as applied questions in material science, engineering as well as biology. Since its invention more than 30 years ago, Atomic Force Microscopy (AFM) has demonstrated the capability of routinely determining structure with sub-nm resolution. Many interesting properties including surface potential [1, 2], electrical conductivity and density of states [3-5] or mechanical parameters [6–8] can be simultaneously measured with AFM. Currently, most AFM measurements of structureproperty relations are slow, on time scales of millisecondshours [9, 10]. Much effort has been put into adding fast time-resolution to understand dynamics and kinetics on time scales of nano- to milliseconds [10-13]. A common assumption in AFM is that the slow time resolution of AFM is related to the mechanical oscillating probe with resonant frequencies of 0.1-1 MHz and slow detection and feedback electronics [14, 15].

In 1990, R. Hamers and D. G. Cahill presented a first approach to ultrafast time resolution in scanning capacitance microscopy with pulsed laser illumination [16, 17]. They pointed out that a time resolution faster than the bandwidth of the detection electronics can be achieved and is only limited by the time response of the underlying physical process of the sample. The proposed idea uses a stimulus S(t) to generate a decaying response in the sample R(S(t)). For a linear responding system, the average signal will correspond to the average of the stimulus. However, for a non-linear response the average of the response $\langle R(S(t)) \rangle$ will depend on the temporal distribution of the stimulating signal, $\langle R(S(t)) \rangle \neq R(\langle S(t) \rangle)$. We will extend this key idea in more general terms and thereby establish the lower limit for time resolution of AFM in terms of the minimal measurable energy for frequency modulation (FM) AFM.

In scanning tunneling microscopy fast time resolution in the picosecond range has been achieved by optical pump-probe excitation and non-linear mixing in the tunnel junction [18–24]. Note the important difference between the non-linear mixing in STM and the non-linear response to a stimulus mentioned above used in this study. STM is limited to conducting samples due to the need of a tunnel current, a limitation not existing for AFM. In addition, small perturbations of the tunnel gap as a result of synchronous thermal expansion is a cause of potential artifacts. Fast time resolution in AFM was achieved in 2015 by Jahng et al. to measure the dynamics in silicon naphtalocyganine using a technique named photo induced force microscopy (PIFM) [25]. PIFM measures the force generated by the light induced dipoles in the tip and sample. This indicates a great potential for extending AFM capabilities to measure fast processes. However, PIFM is limited to the near field dipole interaction between the tip and the sample induced by an optical pulse.

In the following, we will describe how to generically measure a signal decaying in time (i.e. a non-linear signal) with frequency modulation AFM (FM-AFM). This general analysis is not limited to a specific response or time constant and can, therefore, be applied to any timescales and any stimulating signal measured by a mechanical oscillator. It will also allow us to understand what determines the ultimate limitations of time resolution measurements by AFM.

THE LOWER LIMIT FOR TIME RESOLUTION IN AFM

Most sub-nm structural determination by AFM is performed in the FM-AFM mode, where the resonance frequency shift of the oscillating cantilever is a measure of the tip-sample interaction [26].

To measure the frequency shift of a cantilever one has to measure at least half a cycle of oscillation, $T_0/2$. Consequently, one would assume that any changes faster than T_0 would not be resolvable in the frequency shift in real

^{*} zenos@physics.mcgill.ca

time. In the following, we will discuss how to overcome this apparent limitation. To generalize the discussion, we will apply our analysis to a generic time dependent potential energy U(t) of the AFM cantilever. The change in U(t) due to the time dependent tip-sample interaction $U_{\rm ts}(t)$ will translate to a measurable frequency shift [27–30].

Following the approach of Hamers and Cahill [16], an external signal S(t) is applied to modulate the potential energy of the harmonic oscillator U(t) through modulating $U_{ts}(t)$. In FM-AFM, such modulations are often sine waves, e.g. in Kelvin Probe Force Microscopy (KPFM), an AC voltage is applied to modulate the electrostatic F_{ts} . In the following, we will apply a pulsed signal to modulate the tip-sample potential. The modulation signal can be of any nature including electrical, thermal, magnetic or optical, as long as it generates a modulation of the potential energy U which translates to a modulation of the force and force gradient.

Assume two pulse trains which can be delayed in time with respect to each other. Additionally the second pulse train (probe pulse) is modulated to achieve a baseline/differential measurement. Each pulse will lead to an increase of the tip-sample interaction energy and a change in the energy of the harmonic oscillator U followed by a characteristic decay time:

$$\Delta U(S(t)) = \begin{cases} U_0 & \text{for } 0 < t < T_p, \\ U_0 e^{-(t-T_p)/\tau} & \text{for } T_p < t < T_{rep}, \end{cases}$$
(1)

with a pulse duration of T_p , a response amplitude U_0 and a repetition rate of $1/T_{rep}$.

The decay time τ is the property of interest which we want to measure with AFM. In the following we will focus on the case when the decay and pulse width are shorter than the cantilever oscillation period of 1-10 μ sec (and thus substantially shorter than the AFM electronic response time limited by the frequency detector, typically phase-locked loop (PLL), whose bandwidth is typically less than 1 ms). Since the time constant τ can be recovered from the average signal, the cantilever itself can be used as an averaging tool. The only necessary requirement is that the cantilever is capable of resolving the change in potential energy between two different time delay settings. The lower limit for this is given by the minimal detectable energy as described by Albrecht et al. [26] and Smith [31].

The averaged potential energy over one cycle of T_{rep} is calculated below. Considering only terms of the average potential energy which depend on the time delay we find the following expression:

$$\langle \Delta U(S(t)) \rangle = \frac{\tau U_0}{T_{rep}} (1 - e^{-T_d/\tau} - e^{-(T_{rep} - T_d - 2T_p)/\tau}).$$
(2)

The last term in equation 2 can be neglected by implementing a repetition time T_{rep} that is much larger than the pulse width, the delay and the decay time. The remaining expression now allows us to determine the minimum measurable time constant τ in terms of the minimal detectable energy by AFM. Therefore, it is no longer a question of how fast the measurement can be done, but rather how small of a potential energy change can be measured. To determine this, we recall the well-known expression of the thermal limit of AFM [26]. By equating the thermal noise dominated minimum measurable energy for on resonant detection in AFM to the change in potential energy due to the decay from equation 2), we obtain [31]:

$$\frac{\tau U_0}{T_{rep}} (1 - e^{-T_d/\tau}) = \frac{2k_B T}{\pi f_0 Q \tau_s}$$
(3)

with the resonance frequency f_0 , the Q-factor of the cantilever Q, the Boltzmann constant, k and temperature T. τ_s is the integration time (proportional to the inverse of the bandwidth) used in the experiment. Inspecting equation 3 we observe that our average potential energy and thus signal increases with higher repetition rate (i.e. shorter time between pulse pairs) since the system is pumped more often. The signal also depends on the initial response amplitude U_0 . Thus, having a large response to the simulating signal is obviously beneficial. The faster the signal decays (smaller τ), the smaller the averaged measured potential energy change.

Assuming $T_d \ll \tau$, the minimum decay time constant is equal to:

$$\tau = \frac{T_{rep}}{U_0(1 - e^{-\beta})} \frac{2k_B T}{\pi f_0 Q \tau_s} \tag{4}$$

with $\beta = T_d/\tau$, e.g. the ratio between the delay time and the decay time constant.

Note that we chose the simplification of having the same response amplitude for both the pump and probe pulses. This would be the case when the stimulation is saturating the signal, e.g. exciting all carriers in the probe volume. Further analysis can be found in the supplementary information, discussing a variable response amplitude dependent on the delay time, like ground state bleaching. The end result presented here, however, holds in all cases.

EXPERIMENTAL IMPLEMENTATION

The proposed modulation scheme shown in figure 1 is generic and can be implemented with an arbitrary pump and probe signal. Any stimulating signal leading to a decay, which can be applied as a pulse train, can be used. To determine decay times, two pulse trains are needed that can be delayed in time with respect to each other.

We experimentally demonstrate the implementation and measurement by AFM of ultrafast photocarrier decay times in low temperature grown GaAs (LT-GaAs). LT-GaAs has a carrier lifetime in the low picosecond regime, depending on the growth conditions [32]. During the LT growth process, many point defects are created [33, 34]. These defects lead to a short diffusion length of the injected charge carrier and hence a short lifetime. For our measurement, we used a LT-GaAs sample (TeTechS Inc., Ontario, Canada) with a carrier lifetime of about 1 ps. A 1.5 μ m LT-GaAs layer was grown on a 200 nm AlAs etch stop layer. The substrate consists of approximately 600 μ m thick semi-insulating GaAs. The LT-GaAs layer is thicker than the penetration depth of the used illumination and therefore no contribution of the substrate is expected. The penetration depth was calculated to be 653 nm for an illumination with 780 nm and 253 nm for illumination with a 610 nm wavelength, respectively [35].

Our UHV AFM setup based on a JEOL 4500 SPM system was combined with an ultrafast pumped laser source. Commercial Pt coated cantilevers (PPP-NCHPt, Nanosensors) are used ($f_0 = 279647 \text{ Hz}, Q = 11860$). An oscillation amplitude of 6 nm was typically used with the contact potential difference (CPD) compensated. The tip was lifted by 1 nm from a -2 Hz frequency shift setpoint with an applied tip bias of -950 mV with respect to the CPD between tip and sample. A 780 nm laser (Toptica FemtoFiber Pro NIR,80.1 MHz, 94 fs pulse width) is used with a power of 29.8 mW (0.182 nJ/cm^2) and a tunable visible wavelength laser (Toptica FemtoFiber Pro TVIS, 80.1 MHz, 0.4 ps) is adjusted to a 610 nm wavelength with an average power of 5.125 mW (0.032) nJ/cm^2). The fluence is low enough to avoid excessive heating of the AFM tip [36]. The 610 nm beam is chopped at a low frequency (233 Hz) to generate a modulation of the frequency shift. Both lasers are locked to the same repetition rate with the variable repetition rate (VAR) and Laser repetition rate control (LRC) option from Toptica included in the NIR FemtoFiber Pro. A delay between the lasers can be adjusted electronically by adding a phase offset to the phase lock loop. This electronically controlled delay was used to delay the two laser pulses relative to each other. The RMS-jitter of the two locked lasers is measured to be 130 fs.

To measure the average signal generated by the delayed pulse trains, the probe pulse is chopped which translates into a modulation of the frequency shift. Here, the modulation of the frequency shift is measured with either a gated integration setup or a direct sideband lock-in detection [37]. The chopping of the probe beam enables an accurate and drift-free measurement of the electrostatic tip-sample interaction and thus allows the measurement of the decay of photo-excited charges [38].

It is important to note that the chopping of the probe beam needs to be slow enough to be resolved by the PLL. Otherwise, the measured signal will either be influenced by the PLL dynamics or not reach the steady state signal. The frequency shift can then be integrated over a short time interval when no transient effects from the PLL are present. Having a boxcar integration with baseline subtraction allows for the direct measurement of the probe beam effect (see equation 2). This difference will decay with the sought after characteristic time constant τ while the delay between the two pulse trains is swept across the range of interest.

A lock-in measurement at the probe pulse chopping frequency gives information about the difference between the two stages, hence the decay times. For imaging purposes, such a measurement might be well suited. However, if more information needs to be extracted from the change in signal, such as the change in capacitance gradient shown by time domain (TD)-KPFM [38], only a gated integration in the time domain will provide this additional information.

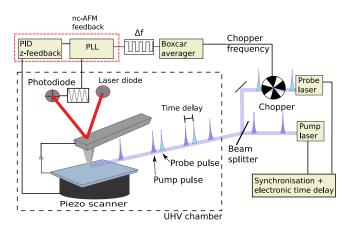


FIG. 1: A pump pulse train (blue) and a probe pulse train (green) are delayed with respect to each other. The probe pulse train is additionally modulated by a chopper. The final pulse train pattern consists of the delay pulse trains with and without the probe beam present. The sample and cantilever react to this pulse train resulting in a modulation of the frequency shift.

A UHF lock-in amplifier from Zurich Instruments with the boxcar averaging option is used for data acquisition. All sideband lock-in measurements are performed with a HF2PLL from Zurich Instruments with direct sideband detection. To verify the change in CPD under pulsed illumination, the LT-GaAs sample is illuminated with 780 nm and TD-KPFM is used to measure the surface photovoltage under pulsed illumination [38]. A surface photovoltage of 96 ± 8 mV is measured for this sample (see figure 2).

The recorded change in frequency shift at constant bias as a function of the delay time between the two laser pulses is plotted in figure 3. The direct sideband detection is performed simultaneously with the boxcar averaging. The data was fitted with a simple exponential decay since a low fluence is used [33, 39]. A decay time of $\tau = 1.1 \pm 0.4$ ps for the sideband detection and $\tau = 0.9 \pm 0.6$ ps for the time domain boxcar averaging is measured by fitting an exponential decay in the form of $a(1 - \exp(-x/\tau)) + c$. This lifetime is in the ex-

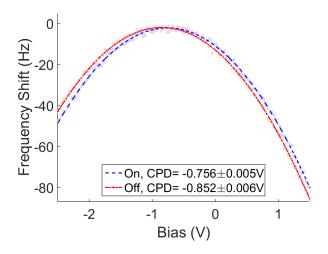


FIG. 2: Surface photovoltage of Lt-GaAs measured with TD-KPFM. A surface photovoltage of 96 ± 8 mV is measured.

pected range of 1 ps within error for both measurements. The fitting term c corresponds to the value at zero delay, hence the first term from equation 2. The term a is equal to the increase in signal between zero delay and the steady state reached after the exponential decay. The data shown in figure 3 is recorded in a similar way to the bias curves previously shown. The tip is lifted by 1 nm, the feedback is turned off and a DC-bias is applied. With the feedback off, the delay between the two laser pulses is scanned and the change in frequency shift is recorded.

In general, the sideband detection appears to have a better signal-to-noise ratio due to the use of a lock-in measurement. Additionally, the upper sideband and the lower sideband are added to increase the signal-to-noise ratio. Sideband detection is also favored for imaging applications. On this sample of LT-GaAs we did not find a spatial variation of τ . This is not surprising given the high density of defects in this sample. In general, as the origin of the tip-sample interaction is electrostatic, the best lateral resolution we expect is similar to KPFM and thus at the nm scale [1].

CONCLUSION

We have derived the fundamental factors determining the fastest possible time resolution of AFM. Surprisingly, time resolution in AFM for a time decaying tip-sample interaction is limited by the thermal noise of the cantilever and not the cantilever mechanical response time or electronic limits of the AFM. We theoretically describe a generic pump-probe scheme with two excitation pulse trains delayed relative to each other that allow for decay time measurements of arbitrary signals and conclude that time resolution is practically limited only by the smallest delay time achievable between the pump and

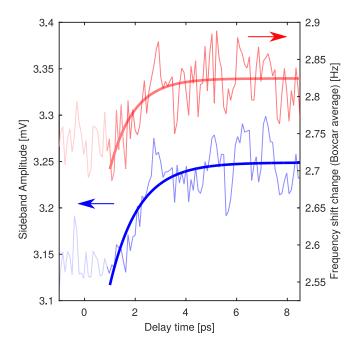


FIG. 3: Photocarrier decay measured in LT-GaAs at constant height (1 nm tip lift) and -950 mV bias. A 780 nm pump laser and a 610 nm probe laser is used.

Decay time recording using the direct sideband detection (blue) compared to the boxcar averaging in the time domain (red) is shown. The decay is fitted to an exponential decay with a time constant of $\tau = 1.1 \pm 0.4$ ps for sideband and $\tau = 0.9 \pm 0.6$ ps for boxcar detection)

probe pulse. This opens the possibility to measure decay times orders of magnitudes faster than the slow mechanical or electrical characteristic times intrinsic to AFM. We experimentally implement this detection scheme by combining a UHV AFM system with a fs pump-probe laser system to measure the ~ 1 ps photocarrier lifetime in LT-GaAs. We have thus achieved a time resolution in AFM which is 10^7 times faster than the oscillation period of the cantilever and 10^{10} times faster than the inverse electronic measurement bandwidth. We emphasize that this pump-probe scheme is not limited to optical excitation as long as the response exhibits a decay with time. Repetitive short pump and probe pulse on the order of the decay time and variable delay times smaller than the decay time is all that is needed. Suitable pump-probe excitation schemes can be envisioned for the investigation of the spatial and time resolved dynamics in photoelectric charge generation and recombination, ion mobility or heat transport. Compared to similar techniques such as PIFM, NSOM or STM a major advantage of the presented AFM technique is that it does not need to operate in the near field and is thus less susceptible to spurious artifacts because the measured interaction signal is not exponentially dependent on tip-sample separation.

ACKNOWLEDGMENTS

The authors would like to thank Prof. David Cook and Prof. Carlos Silva for extensive scientific discussion. The authors would like to thank the NSERC and FQRNT for funding. Z.S. would like to thank the SNSF for a DOC.Mobility fellowship.

- [1] L. Gross, B. Schuler, F. Mohn, N. Moll, N. Pavliček, W. Steurer, I. Scivetti, K. Kotsis, M. Persson, and G. Meyer, "Investigating atomic contrast in atomic force microscopy and Kelvin probe force microscopy on ionic systems using functionalized tips," *Physical Review B*, vol. 90, p. 155455, oct 2014.
- [2] B. Schuler, S.-X. Liu, Y. Geng, S. Decurtins, G. Meyer, and L. Gross, "Contrast formation in Kelvin probe force microscopy of single π-conjugated molecules.," *Nano letters*, vol. 14, pp. 3342–6, jun 2014.
- [3] J. G. Park, S. H. Lee, B. Kim, and Y. W. Park, "Electrical resistivity of polypyrrole nanotube measured by conductive scanning probe microscope: The role of contact force," *Applied Physics Letters*, vol. 81, no. 24, p. 4625, 2002.
- [4] L. S. C. Pingree, O. G. Reid, and D. S. Ginger, "Electrical Scanning Probe Microscopy on Active Organic Electronic Devices," *Advanced Materials*, vol. 21, pp. 19–28, jan 2009.
- [5] A. Roy-Gobeil, Y. Miyahara, and P. Grutter, "Revealing Energy Level Structure of Individual Quantum Dots by Tunneling Rate Measured by Single-Electron Sensitive Electrostatic Force Spectroscopy," *Nano Letters*, vol. 15, pp. 2324–2328, apr 2015.
- [6] E. Gnecco and E. Meyer, Fundamentals of Friction and Wear on the Nanoscale. NanoScience and Technology, Cham: Springer International Publishing, 2015.
- [7] R. Bennewitz, "Friction force microscopy," Materials Today, vol. 8, pp. 42–48, may 2005.
- [8] W. Paul, D. Oliver, and P. Grütter, "Indentation-formed nanocontacts: an atomic-scale perspective," *Physical Chemistry Chemical Physics*, vol. 16, no. 18, p. 8201, 2014.
- [9] A. Schirmeisen, A. Taskiran, H. Fuchs, B. Roling, S. Murugavel, H. Bracht, and F. Natrup, "Probing ion transport at the nanoscale: Time-domain electrostatic force spectroscopy on glassy electrolytes," *Applied Physics Letters*, vol. 85, no. 11, p. 2053, 2004.
- [10] D. C. Coffey and D. S. Ginger, "Time-resolved electrostatic force microscopy of polymer solar cells," *Nature Materials*, vol. 5, pp. 735–740, sep 2006.
- [11] M. Takihara, T. Takahashi, and T. Ujihara, "Minority carrier lifetime in polycrystalline silicon solar cells studied by photoassisted Kelvin probe force microscopy," *Applied Physics Letters*, vol. 93, no. 2, p. 021902, 2008.
- [12] G. Shao, M. S. Glaz, F. Ma, H. Ju, and D. S. Ginger, "Intensity-Modulated Scanning Kelvin Probe Microscopy for Probing Recombination in Organic Photovoltaics," ACS Nano, vol. 8, no. 10, pp. 10799–10807, 2014.
- [13] D. U. Karatay, J. S. Harrison, M. S. Glaz, R. Giridharagopal, and D. S. Ginger, "Fast time-resolved electrostatic force microscopy: Achieving sub-cycle time

resolution," *Review of Scientific Instruments*, vol. 87, p. 053702, may 2016.

- [14] T. Ando, "High-speed atomic force microscopy coming of age," *Nanotechnology*, vol. 23, p. 062001, feb 2012.
- [15] T. Ando, T. Uchihashi, and T. Fukuma, "High-speed atomic force microscopy for nano-visualization of dynamic biomolecular processes," *Progress in Surface Science*, vol. 83, pp. 337–437, nov 2008.
- [16] R. J. Hamers and D. G. Cahill, "Ultrafast time resolution in scanned probe microscopies," *Applied Physics Letters*, vol. 57, no. 19, pp. 2031–2033, 1990.
- [17] R. J. Hamers and D. G. Cahill, "Ultrafast time resolution in scanned probe microscopies: Surface photovoltage on Si(111)-(7x7)," Journal of Vacuum Science & Technology B: Microelectronics and Nanometer Structures, vol. 9, p. 514, mar 1991.
- [18] S. Yoshida, Y. Terada, M. Yokota, O. Takeuchi, H. Oigawa, and H. Shigekawa, "Optical pump-probe scanning tunneling microscopy for probing ultrafast dynamics on the nanoscale," *The European Physical Journal Special Topics*, vol. 222, pp. 1161–1175, jul 2013.
- [19] S. Yoshida, Y. Terada, R. Oshima, O. Takeuchi, and H. Shigekawa, "Nanoscale probing of transient carrier dynamics modulated in a GaAs-PIN junction by lasercombined scanning tunneling microscopy," *Nanoscale*, vol. 4, no. 3, p. 757, 2012.
- [20] Y. Terada, S. Yoshida, O. Takeuchi, and H. Shigekawa, "Real-space imaging of transient carrier dynamics by nanoscale pumpprobe microscopy," *Nature Photonics*, vol. 4, pp. 869–874, oct 2010.
- [21] Y. Terada, S. Yoshida, O. Takeuchi, and H. Shigekawa, "Laser-combined scanning tunnelling microscopy for probing ultrafast transient dynamics," *Journal of Physics: Condensed Matter*, vol. 22, p. 264008, jul 2010.
- [22] S. Yoshida, Y. Aizawa, Z.-H. Wang, R. Oshima, Y. Mera, E. Matsuyama, H. Oigawa, O. Takeuchi, and H. Shigekawa, "Probing ultrafast spin dynamics with optical pump-probe scanning tunnelling microscopy.," *Nature nanotechnology*, pp. 1–6, jun 2014.
- [23] T. L. Cocker, V. Jelic, M. Gupta, S. J. Molesky, J. A. J. Burgess, G. D. L. Reyes, L. V. Titova, Y. Y. Tsui, M. R. Freeman, and F. A. Hegmann, "An ultrafast terahertz scanning tunnelling microscope," *Nature Photonics*, vol. 7, pp. 620–625, jul 2013.
- [24] S. Grafstrom, "Photoassisted scanning tunneling microscopy," *Journal of Applied Physics*, vol. 91, no. 4, p. 1717, 2002.
- [25] J. Jahng, J. Brocious, D. a. Fishman, S. Yampolsky, D. Nowak, F. Huang, V. a. Apkarian, H. K. Wickramasinghe, and E. O. Potma, "Ultrafast pump-probe force microscopy with nanoscale resolution," *Applied Physics Letters*, vol. 106, p. 083113, feb 2015.
- [26] T. R. Albrecht, P. Grütter, D. Horne, and D. Rugar, "Frequency modulation detection using high-Q cantilevers for enhanced force microscope sensitivity," *Journal of Applied Physics*, vol. 69, p. 668, jan 1991.
- [27] U. Durig, "Relations between interaction force and frequency shift in large-amplitude dynamic force microscopy," *Applied Physics Letters*, vol. 75, no. 3, p. 433, 1999.
- [28] F. J. Giessibl, "Forces and frequency shifts in atomicresolution dynamic-force microscopy," *Physical Review B*, vol. 56, pp. 16010–16015, dec 1997.
- [29] R. García, "Dynamic atomic force microscopy methods," Surface Science Reports, vol. 47, pp. 197–301, sep 2002.

- [30] L. N. Kantorovich and T. Trevethan, "General Theory of Microscopic Dynamical Response in Surface Probe Microscopy: From Imaging to Dissipation," *Physical Review Letters*, vol. 93, p. 236102, nov 2004.
- [31] D. P. E. Smith, "Limits of force microscopy," Review of Scientific Instruments, vol. 66, no. 5, p. 3191, 1995.
- [32] S. Gupta, M. Y. Frankel, J. A. Valdmanis, J. F. Whitaker, G. A. Mourou, F. W. Smith, and A. R. Calawa, "Subpicosecond carrier lifetime in GaAs grown by molecular beam epitaxy at low temperatures," *Applied Physics Letters*, vol. 59, no. 25, p. 3276, 1991.
- [33] G. Segschneider, F. Jacob, T. Löffler, H. G. Roskos, S. Tautz, P. Kiesel, and G. Döhler, "Free-carrier dynamics in low-temperature-grown GaAs at high excitation densities investigated by time-domain terahertz spectroscopy," *Physical Review B*, vol. 65, p. 125205, mar 2002.
- [34] E. S. Harmon, M. R. Melloch, J. M. Woodall, D. D. Nolte, N. Otsuka, and C. L. Chang, "Carrier lifetime versus anneal in low temperature growth GaAs," *Applied Physics Letters*, vol. 63, no. 16, p. 2248, 1993.

- [35] G. Jellison, "Optical functions of GaAs, GaP, and Ge determined by two-channel polarization modulation ellipsometry," *Optical Materials*, vol. 1, pp. 151–160, sep 1992.
- [36] A. a. Milner, K. Zhang, V. Garmider, and Y. Prior, "Heating of an Atomic Force Microscope tip by femtosecond laser pulses," *Applied Physics A*, vol. 99, pp. 1–8, apr 2010.
- [37] U. Zerweck, C. Loppacher, T. Otto, S. Grafström, and L. M. Eng, "Accuracy and resolution limits of Kelvin probe force microscopy," *Physical Review B*, vol. 71, p. 125424, mar 2005.
- [38] Z. Schumacher, Y. Miyahara, A. Spielhofer, and P. Grutter, "Measurement of Surface Photovoltage by Atomic Force Microscopy under Pulsed Illumination," *Physical Review Applied*, vol. 5, no. 4, p. 044018, 2016.
- [39] K. a. McIntosh, K. B. Nichols, S. Verghese, and E. R. Brown, "Investigation of ultrashort photocarrier relaxation times in low-temperature-grown GaAs," *Applied Physics Letters*, vol. 70, no. 3, p. 354, 1997.